Disruption of Mouse *RAD54* Reduces Ionizing Radiation Resistance and Homologous Recombination

Jeroen Essers,* Rudolf W. Hendriks,*
Sigrid M. A. Swagemakers,* Christine Troelstra,*†
Jan de Wit,* Dirk Bootsma,*
Jan H. J. Hoeijmakers,* and Roland Kanaar*†
*Medical Genetics Center
Department of Cell Biology and Genetics
Erasmus University Rotterdam
3000 DR Rotterdam
The Netherlands
†Department of Radiotherapy
Division of Clinical Radiobiology
Dr. Daniël den Hoed Center
3075 EA Rotterdam
The Netherlands

Summary

Double-strand DNA break (DSB) repair by homologous recombination occurs through the *RAD52* pathway in Saccharomyces cerevisiae. Its biological importance is underscored by the conservation of many *RAD52* pathway genes, including *RAD54*, from fungi to humans. We have analyzed the phenotype of mouse *RAD54*$^{-/-}$ (*mRAD54*$^{-/-}$) cells. Consistent with a DSB repair defect, these cells are sensitive to ionizing radiation, mitomycin C, and methyl methanesulfonate, but not to ultraviolet light. Gene targeting experiments demonstrate that homologous recombination in *mRAD54*$^{-/-}$ cells is reduced compared to wild-type cells. These results imply that, besides DNA end-joining mediated by DNA-dependent protein kinase, homologous recombination contributes to the repair of DSBs in mammalian cells. Furthermore, we show that *mRAD54*$^{-/-}$ mice are viable and exhibit apparently normal V(D)J and immunoglobulin class-switch recombination. Thus, *mRAD54* is not required for the recombination processes that generate functional immunoglobulin and T cell receptor genes.

Introduction

Double-strand DNA breaks (DSBs) are induced by ionizing radiation, which is often used in cancer therapy, and by radiomimetic agents including endogenously produced radicals. Accurate repair of these genotoxic lesions is essential for the prevention of chromosomal fragmentation, translocations, and deletions. All of these forms of genomic instability can lead to carcinogenesis through activation of oncogenes, inactivation of tumor suppressor genes, or loss of heterozygosity. Insight into the mechanisms of DSB repair in mammals is crucial for an understanding of the biological consequences of exposure to ionizing radiation.

Mutants in the Saccharomyces cerevisiae *RAD52* epistasis group are defective in DSB repair through homologous recombination and display sensitivity to ionizing radiation and the alkylating agent methyl methanesulfonate (MMS) (Game, 1993; Haber, 1995). Recently,

it has become clear that the primary sequence of many *RAD52* group genes is conserved from yeast to humans (Petrini et al., 1997). Key genes in the *RAD52* DNA repair pathway include *RAD51* and *RAD54*. Biochemical experiments have demonstrated that Rad51 protein and its human counterpart, hRad51, are functional homologs of the Escherichia coli recombination protein RecA. These proteins form nucleoprotein filaments with single-stranded DNA and mediate homologous DNA pairing and strand exchange (Ogawa et al., 1993; Benson et al., 1994; Sung, 1994; Sung and Robberson, 1995; Baumann et al., 1996; Gupta et al., 1997). Genetic experiments with yeast have revealed that Rad54 and its human counterpart, hRad54, are functional homologs with respect to the repair of MMS-induced DNA damage (Kanaar et al., 1996). The proteins belong to the SNF2/SWI2 family of DNA-dependent ATPases (Eisen et al., 1995). Its members have been implicated in the remodeling of chromatin structure in the context of many aspects of DNA metabolism such as transcription, recombination, and repair (Kingston et al., 1996). Rad54 might function together with Rad51 since genetic and physical interactions between these two S. cerevisiae proteins have been observed (Jiang et al., 1996; Clever et al., 1997).

Mechanisms of mammalian DSB repair have been investigated with the use of a collection of ionizing radiation–sensitive Chinese hamster cell lines (Jeggo, 1990). A number of these cell lines have specific defects in DSB repair, and the correcting genes have been identified. Genetic and biochemical analyses have revealed that these cell lines are defective in DNA end-joining that requires no or extremely limited DNA homology (Jeggo et al., 1995; Roth et al., 1995). Proteins involved in this pathway include the subunits of DNA-dependent protein kinase (DNA-PK): the DNA-PK catalytic subunit (DNA-PK$_{cs}$) and the Ku70/80 heterodimer, which has DNA end-binding activity. In contrast to the plethora of yeast mutants, there are no mammalian mutant cell lines with documented defects in homologous recombination. Therefore, while the contribution of homologous recombination to ionizing radiation resistance in yeast is well established, its contribution in mammals is unknown.

Recently, it has been established that many of the proteins involved in DNA end-joining are also required for immunoglobulin and T cell receptor (TCR) gene rearrangement (Jeggo et al., 1995; Roth et al., 1995). Two types of DNA rearrangements lead to the production of functional immunoglobulin genes during B cell development. The first is V(D)J recombination, which determines the antigenic specificity of the encoded antibody. It occurs at recombination signal sequences and is initiated by a site-specific DSB introduced by the RAG1 and RAG2 proteins (Gellert, 1996). Additional proteins required for V(D)J recombination include DNA-PK and XRCC4 (Gellert, 1996). Functional TCR genes are also assembled through V(D)J recombination. The second DNA rearrangement is immunoglobulin class-switch recombination, which changes the constant region of the immunoglobulin heavy (H) chain, thereby switching the isotype of the encoded antibody (Harriman et al., 1993).

While the early immune response in mice is dominated by expression of immunoglobulin M (IgM) and IgD, class-switch recombination allows expression of IgG1, IgG2a, IgG2b, IgG3, IgA, and IgE. Class-switch recombination is more reminiscent of homologous recombination than of site-specific recombination, because it involves switch regions that vary between 2 and 10 kb and contain a large array of short repeated sequences. In contrast to V(D)J recombination, enzymatic activities required for class-switch recombination have not yet been identified. Since the expression of all mammalian *RAD52* group genes, isolated to date, is increased in organs of lymphoid development, it is of considerable interest to determine whether they are involved in immunoglobulin and TCR gene rearrangements.

To address whether recombinational repair contributes to ionizing radiation resistance in mammals, we have generated mouse embryonic stem (ES) cells in which both alleles of *mRAD54* have been disrupted. These cells have a reduced level of homologous recombination as measured by gene targeting. This observation provides genetic evidence for the functional conservation of the *RAD52* homologous recombination pathway in mammalian cells. Significantly, *mRAD54*$^{-/-}$ cells display sensitivity to ionizing radiation, mitomycin C, and MMS compared to otherwise isogenic wild-type and heterozygous mutant cell lines. These results suggest that besides DNA end-joining, homologous recombination contributes to ionizing radiation resistance in mammalian cells. To assess the biological impact of homologous recombination at the level of the intact organism, we generated *mRAD54*$^{-/-}$ mice. In contrast to inactivation of the *mRAD51* gene, which causes an embryonic lethal phenotype (Lim and Hasty, 1996; Tsuzuki et al., 1996), *mRAD54*$^{-/-}$ mice are viable. Analyses of cell surface markers, indicative of V(D)J recombination, on cells isolated from thymus, bone marrow, peritoneal cavity, and spleen have not revealed a difference between *mRAD54*$^{+/+}$ and *mRAD54*$^{-/-}$ mice. In addition, the level of different immunoglobulin subclasses in the serum of mutant mice is similar to that found in wild-type mice. These results show that *mRAD54* is not required for V(D)J and immunoglobulin class-switch recombination.

Results

Generation of *mRAD54*-Disrupted Mouse Cells

We generated mouse ES cells lacking mRad54 to determine the phenotype of a mammalian *RAD54* mutant. Using the *mRAD54* cDNA as a probe, the *mRAD54* genomic locus was isolated by screening a lambda and a cosmid library made from strain 129/Sv genomic DNA. Three clones that spanned the approximately 30 kb *mRAD54* genomic locus (Figure 1A) were obtained. The locus was extensively characterized by restriction site mapping and sequencing of intron–exon borders. The EcoRI fragment containing exon 4 was subcloned and disrupted by insertion of selectable marker genes at a position corresponding to nucleotide position 307 in the *mRAD54* cDNA. The insertion results in elimination of 90% of the protein, including all seven highly conserved

motifs implicated in the essential DNA-dependent ATPase activity. Moreover, aberrant RNA splicing that skips the targeted exon would result in a frameshift mutation. Three disruption constructs containing the neomycin-, hygromycin-, and puromycin-selectable markers were made. They are referred to as *mRAD54*^{307neo}, *mRAD54*^{307hyg}, and *mRAD54*^{307pur}, respectively.

The *mRAD54*^{307neo} construct was electroporated into E14 ES cells. After selection, targeted clones were identified by DNA blotting using a unique probe outside the targeting construct (Figure 1B). Multiple independent cell lines containing one disrupted *mRAD54* allele were obtained at a frequency of approximately 40%. The second wild-type allele was disrupted by targeting with either the *mRAD54*^{307hyg} or the *mRAD54*^{307pur} construct. Several double-knockout cell lines in which the remaining wild-type allele was replaced by *mRAD54*^{307hyg} or *mRAD54*^{307pur}, respectively, were obtained. In addition, heterozygous mutant cell lines in which the targeting constructs had replaced the previously targeted *mRAD54*^{307neo} allele instead of the wild-type allele (Figure 1B) were obtained. No significant difference in growth rate between *mRAD54*$^{+/+}$ ES cells and all of the different *mRAD54*$^{+/-}$ and *mRAD54*$^{-/-}$ ES cell lines was detected (data not shown). We conclude that, similar to the situation in S. cerevisiae and Schizosaccharomyces pombe (Muris et al., 1996), disruption of the *RAD54* homolog in mouse cells results in viable cells.

We next investigated the consequence of disrupting *mRAD54* at the protein level. The *mRAD54* cDNA encodes a protein of 747 amino acids with a predicted molecular weight of 84.6 kDa. The human homolog of mRad54 is 94% identical and migrates at this predicted molecular weight (Kanaar et al., 1996; data not shown). A protein of the expected molecular weight was detected in extracts from HeLa cells and from wild-type and *mRAD54*$^{+/-}$ mouse ES cells by immunoblotting using affinity-purified anti-hRad54 antibodies (Figure 1C). In contrast, the protein could not be detected in *mRAD54*$^{-/-}$ ES cells. The nature of the 110 kDa protein that cross-reacted with the anti-hRad54 antibodies is unknown. In addition, RNA blotting experiments showed that the *mRAD54* transcript, though present in *mRAD54*$^{+/+}$ and *mRAD54*$^{+/-}$ ES cells, was not detectable in *mRAD54*$^{-/-}$ ES cells (data not shown). We conclude that disruption of both copies of *mRAD54* exon 4 results in an *mRAD54* null mutation.

mRAD54$^{-/-}$ ES Cells Are Sensitive to Ionizing Radiation and MMS

S. cerevisiae *RAD52*-group mutants, including *rad54Δ*, are sensitive to ionizing radiation and MMS. We therefore investigated the effect of these DNA-damaging agents on *mRAD54*$^{-/-}$ ES cells. They were found to be approximately 2.3-fold more sensitive to γ-irradiation than *mRAD54*$^{+/+}$ and *mRAD54*$^{+/-}$ cells (Figure 2A). In this experiment and all others described in this article, no significant difference was found between wild-type and heterozygous mutant cells. In addition, *mRAD54*$^{-/-}$ cells were found to be 3- to 4-fold more sensitive to MMS than *mRAD54*$^{+/+}$ and *mRAD54*$^{+/-}$ cells (Figure 2B). These results are consistent with the notion that S.
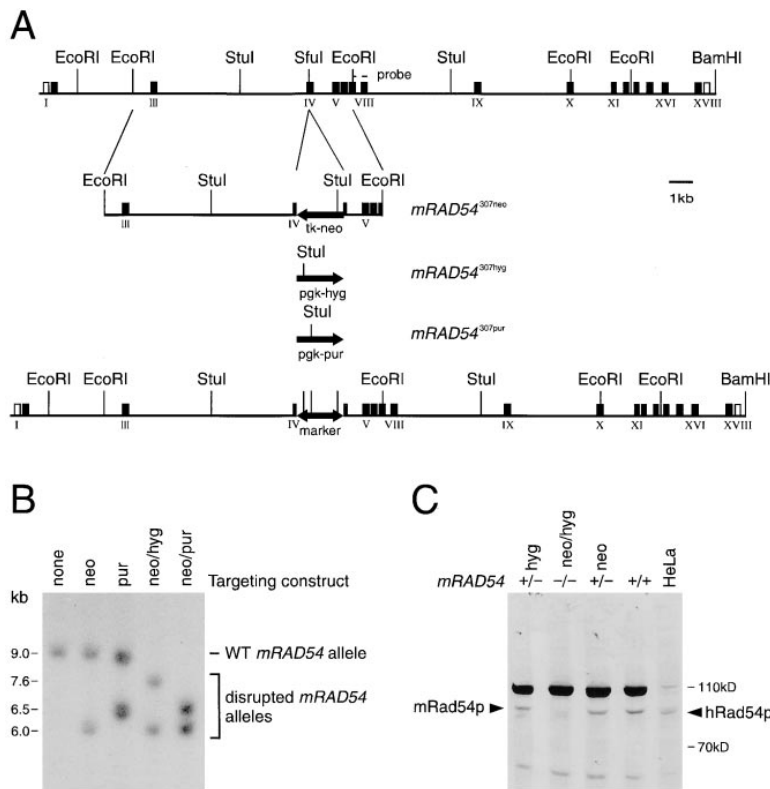
Figure 1. Characterization of the *mRAD54* Genomic Locus and Generation of *mRAD54*-Disrupted Mouse ES Cells

(A) Structure of the genomic *mRAD54* locus and gene targeting constructs. The top line represents the approximately 30 kb *mRAD54* genomic locus. All 18 exons that make up the *mRAD54* cDNA are indicated by boxes. The exons containing the start and stop codons are represented by open boxes. The dashed line above exons 7 and 8 indicates the position of the probe used to screen for the disrupted allele. Shown are the locations of selected restriction sites. The middle line represents the targeting constructs and shows the position of the selectable marker genes neomycin (*neo*), hygromycin (*hyg*), and puromycin (*pur*) in exon 4. The disrupted genomic locus is represented by the bottom line. The vertical lines in the double-headed arrow indicate the relative position of the diagnostic StuI site in the three marker genes. (B) DNA blot of *mRAD54* wild-type and mutant ES cells. ES cells were electroporated with the three different targeting constructs. Genomic DNA was isolated from individual clones and digested with StuI. Clones containing the homologously integrated targeting constructs were identified by DNA blotting using the probe indicated in (A). Heterozygous mutant cell lines containing the *mRAD54^(307neo)* allele were subsequently targeted with the *mRAD54^(307hyg)* and *mRAD54^(307pur)* targeting constructs to generate *mRAD54^(−/−)* cell lines.

(C) Immunoblot of protein extracts from *mRAD54* wild-type and mutant ES cells. Protein extracts from *mRAD54^(+/+)*, *mRAD54^(+/−)*, *mRAD54^(−/−)*, and HeLa cells were separated on an 8% SDS–polyacrylamide gel electrophoresis gel, transfered to nitrocellulose, and hybridized with affinity-purified anti-hRad54 antibodies. Detection was performed with alkaline phosphatase–coupled goat anti-rabbit antibodies. The sizes of the protein molecular weight markers are indicated in kilodaltons on the right. The arrowheads indicate the position of the mammalian Rad54 proteins.

cerevisiae *RAD54* and *mRAD54* are functional homologs (Kanaar et al., 1996). We conclude that disruption of *RAD54* in S. cerevisiae and in mouse ES cells results in a qualitatively similar phenotype with respect to ionizing radiation and MMS sensitivity.

mRAD54^(−/−) ES Cells Are Sensitive to Mitomycin C but Not to Ultraviolet Light

Mitomycin C introduces interstrand cross-links in DNA (Tomasz et al., 1987). We tested *mRAD54^(−/−)* cells for sensitivity to this agent because DSBs are likely intermediates in the repair of such lesions. *mRAD54^(−/−)* cells were found to be 2- to 3-fold more sensitive to mitomycin C than *mRAD54^(+/+)* and *mRAD54^(+/−)* cells (Figure 3A). To prove that the phenotype of the *mRAD54^(−/−)* cells was caused exclusively by the disruption of *mRAD54*, cDNA rescue experiments were performed. *mRAD54^(307neo/hyg)* cells were electroporated with a cDNA construct expressing mRad54 together with a plasmid expressing the dominant selectable marker puromycin. Puromycin-resistant colonies were characterized by DNA blotting and immunoblot analysis to identify cell lines that stably expressed mRad54 (data not shown). The cDNA construct fully corrected the mitomycin C sensitivity of *mRAD54^(−/−)* ES cells (Figure 3A). To show that the *mRAD54^(−/−)* ES cells were specifically deficient in recombinational DNA repair, we tested the

sensitivity of the cells to ultraviolet (UV) irradiation, which causes damage that is repaired primarily by nucleotide excision repair. No significant difference in sensitivity was detected among *mRAD54^(+/+)*, *mRAD54^(+/−)*, and *mRAD54^(−/−)* ES cells (Figure 3B).

Homologous Recombination in *mRAD54^(−/−)* ES Cells Is Reduced

It is generally believed that homologous recombination, resulting in targeted integration, is relatively rare in mammalian cells compared to illegitimate recombination, resulting in random integration. However, it has previously been demonstrated that homologous rather than illegitimate recombination can be predominant in mammalian cells (te Riele et al., 1992). To test whether *mRAD54* is involved in homologous recombination in mouse ES cells, we performed gene targeting experiments. *mRAD54* wild-type, heterozygous mutant (*mRAD54^(307neo/+)*), and double-knockout (*mRAD54^(307neo/hyg)*) cells were electroporated with a construct designed to target the mouse *CSB* locus (van der Horst et al., 1997). This targeting construct is referred to as *CSB-pur* since it contains a phosphoglycerate kinase (PGK) promoter-driven puromycin resistance gene as a dominant selectable marker. The total number of puromycin-resistant colonies obtained was similar for each genotype (see legend to Table 1). Genomic DNA was isolated
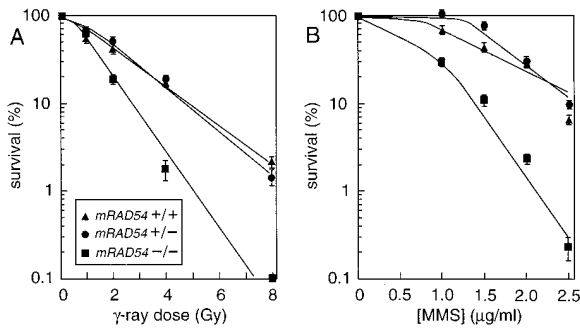
Figure 2. Effect of Ionizing Radiation and MMS on Wild-type and Mutant *mRAD54* ES Cells

(A) Clonogenic survival of *mRAD54$^{+/+}$*, *mRAD54$^{+/-}$*, and *mRAD54$^{-/-}$* ES cells after treatment with increasing doses of γ-rays. After irradiation, cells were plated and allowed to form individual colonies. The percentage of surviving cells as measured by their colony-forming ability is plotted as a function of the γ-ray dose. For all survival experiments described in this article, cells were grown for 7–10 days after treatment and subsequently fixed, stained, and counted. Cloning efficiencies varied from 10% to 30%. All measurements were performed in triplicate. Consistent results were obtained among different sets of experiments. The mutant cells used in the survival experiments were *mRAD54$^{307neo/+}$* and *mRAD54$^{307neo/hyg}$*.

(B) Clonogenic survival of *mRAD54$^{+/+}$*, *mRAD54$^{+/-}$*, and *mRAD54$^{-/-}$* ES cells after treatment with increasing concentrations of MMS. Fresh serial dilutions of MMS were prepared in PBS and added to the growth medium for 1 hr, after which the cells were washed twice with PBS and returned to fresh growth medium.

from individual clones and analyzed by DNA blotting to discriminate between homologous and random integration events. Targeting efficiency was measured as the percentage of clones containing the homologously integrated targeting construct relative to the total number of analyzed drug-resistant clones (Table 1). The targeting efficiency of the *CSB-pur* construct was 18% and 20%
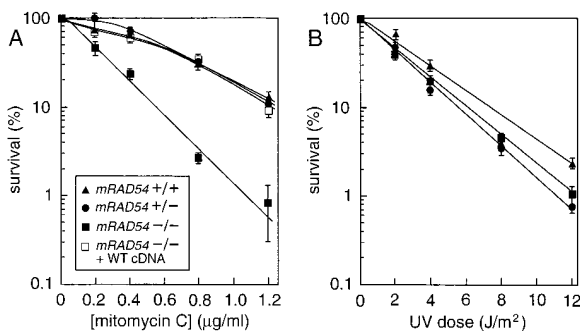

Figure 3. Effect of Mitomycin C and UV Light on Wild-type and Mutant *mRAD54* ES Cells

(A) Clonogenic survival of *mRAD54$^{+/+}$*, *mRAD54$^{+/-}$*, and *mRAD54$^{-/-}$* ES cells after treatment with increasing concentrations of the cross-linking agent mitomycin C and rescue of the mitomycin C sensitivity of *mRAD54$^{-/-}$* cells with an *mRAD54* cDNA expression construct. This survival experiment was performed as described for the MMS treatment. An *mRAD54$^{-/-}$* cell line containing randomly integrated *mRAD54* cDNA expression constructs was obtained as described in Experimental Procedures. Expression of mRad54 in this cell line was verified by immunoblot experiments.

(B) Clonogenic survival of *mRAD54$^{+/+}$*, *mRAD54$^{+/-}$*, and *mRAD54$^{-/-}$* ES cells after treatment with increasing doses of UV light.

Table 1. Homologous Recombination Is Reduced in *mRAD54$^{-/-}$* ES Cells: Percentages of Homologous Integration Events among Total Number of Integration Events

ES Cell Genotype	Targeting Construct		
	CSB-pur	*RB-pur*	*RB-hyg*
mRAD54$^{+/+}$	18% (10/56)	ND	ND
mRAD54$^{neo/+}$	20% (19/95)	20% (19/96)	13% (10/76)
mRAD54$^{neo/hyg}$	4% (3/69)	3% (2/61)	NA
mRAD54$^{neo/pur}$	NA	NA	<1% (0/82)

ES cells of the indicated genotype were electroporated with the indicated targeting constructs. The frequency of drug resistant clones obtained for each genotype was similar. It varied from 2 to 5×10^{-4} for *CSB-pur*, from 2.5 to 3.5×10^{-4} for *RB-pur*, and from 3 to 6×10^{-5} for *RB-hyg*. Values shown are the percentage of clones containing homologously integrated targeting construct relative to the total number of analyzed clones; absolute numbers are given in parentheses. No significant difference in the frequency of homologous integration of *CSB-pur* was observed in the *mRAD54$^{+/+}$* and *mRAD54$^{+/-}$* cell lines (p > 0.5 by chi-squared analysis). In contrast, this frequency was significantly different between those cell lines and the *mRAD54$^{-/-}$* cell line (p < 0.01). The frequency between the *mRAD54$^{+/-}$* and *mRAD54$^{-/-}$* cell lines for *RB-pur* and *RB-hyg* was also significantly different (p < 0.01 and p < 0.005, respectively). ND, not determined; NA, not applicable.

in *mRAD54$^{+/+}$* and *mRAD54$^{307neo/+}$* cells, respectively. In contrast, only 4% of the *mRAD54$^{307neo/hyg}$* puromycin-resistant colonies contained homologously integrated *CSB-pur* DNA.

To exclude the possibility that the reduction of homologous recombination in *mRAD54$^{-/-}$* cells was due to the nature of the *CSB* locus, we performed additional targeting experiments to the mouse *RB* locus, which is unrelated to the *CSB* locus. An *RB-pur* construct had a targeting efficiency of 20% in heterozygous mutant *mRAD54* cells (Table 1). This efficiency was identical to the one found for *CSB-pur*. Significantly, homologous integration of the *RB-pur* construct was reduced approximately 7-fold in *mRAD54$^{-/-}$* cells. In addition, the targeting efficiency of a second *RB* targeting construct (*RB-hyg*) containing the hygromycin resistance gene as selectable marker was determined in an independently obtained *mRAD54$^{-/-}$* cell line (*mRAD54$^{307neo/pur}$*). The targeting efficiency of this construct was more than 10-fold reduced in the *mRAD54$^{-/-}$* cell line compared to the *mRAD54$^{+/-}$* control cell line.

In summary, the gene targeting experiments showed that homologous recombination was reduced in two different targeting loci and in two independently generated *mRAD54$^{-/-}$* cell lines. These experiments provide genetic evidence for involvement of *mRAD54* in homologous recombination in mammalian cells. Interestingly, homologous recombination was not completely inactivated in *mRAD54$^{-/-}$* cells.

Generation of *mRAD54*-Deficient Mice

The experiments described above show that absence of mRad54 is compatible with normal ES cell growth. Subsequently, we investigated whether mRad54 is required for normal mouse development. Two of the targeted ES clones, carrying the *mRAD54^{307neo}* allele, were injected into C57BL/6 blastocysts. One clone transmitted the disrupted *mRAD54* allele to the mouse germline.

Two chimeras transmitted the coat color encoded by the ES cell genome to almost all of their 65 offspring, of which 29 were heterozygous for the disrupted *mRAD54* allele. F1 heterozygous offspring were intercrossed, and F2 offspring were genotyped by DNA blotting or polymerase chain reaction (PCR) analysis or both (data not shown). Among 52 genotyped animals, 12 *mRAD54$^{+/+}$*, 29 *mRAD54$^{+/-}$*, and 11 *mRAD54$^{-/-}$* animals were identified. This outcome is consistent with a normal Mendelian segregation of the disrupted *mRAD54* allele. Thus, an *mRAD54* null mutation does not result in embryonic or neonatal lethality. No statistically significant difference in weight was observed among *mRAD54$^{-/-}$*, *mRAD54$^{+/-}$*, and *mRAD54$^{+/+}$* littermates. Importantly, the *mRAD54$^{-/-}$* mice exhibited no macroscopic abnormalities up to at least 5 months of age.

mRad54 Protein Is Not Required for V(D)J Recombination

To investigate whether *mRAD54* is necessary for the processing of DSBs during V(D)J recombination, we examined the expression of immunoglobulin and TCR genes in the *mRAD54$^{-/-}$* mice by flow cytometry. In the thymus, the total quantity of cells, the CD4/CD8 profile, and the expression of TCRαβ or TCRγδ were normal (Figure 4). In addition, no accumulation of immature Thy-1^{+}/Il-2R^{+} thymocytes, as occurs in RAG1- or RAG2-deficient mice (Mombaerts et al., 1992; Shinkai et al., 1992), was observed in *mRAD54$^{-/-}$* mice, and normal quantities of CD4^{+} and CD8^{+} cells were present in the spleen (data not shown). Thus, TCR expression and the differentiation process leading to the generation of mature single-positive T cells occurs efficiently in the absence of mRad54.

B cell development was studied by analysis of surface expression of B220, CD43, IgM, and IgD, which resolve B cell progenitors into discrete stages (Hardy et al., 1991). No differences among *mRAD54$^{+/+}$*, *mRAD54$^{+/-}$*, and *mRAD54$^{-/-}$* mice were observed in the various B cell progenitors in the bone marrow. The transition of B220^{+}CD43^{+} pro–B cells to B220^{+}CD43^{-} pre–B cells, which marks the completion of functional immunoglobulin H V(D)J recombination, is not affected by the absence of mRad54 (Figure 4). In the peritoneal cavity the quantity of conventional B cells and CD5^{+} B cells was in the normal range (data not shown). In addition, the quantity of B cells in the spleen and their IgM/IgD profiles were normal (Figure 4). These results show that mRad54 is not essential for V(D)J recombination.

mRad54 Protein Is Not Required for Immunoglobulin H Chain Class-Switch Recombination

B cells can join the V(D)J exon to different downstream effector H chain constant regions by recombination between repetitive switch regions present 5' of each germline H chain constant region. To investigate whether *mRAD54* is involved in the immunoglobulin H chain class-switch recombination from IgM to IgG, IgA and IgE, we determined the levels of immunoglobulin subclasses in the serum using an enzyme-linked immunosorbent assay (ELISA). The concentrations of IgM as well as the concentrations of secondary isotypes, including
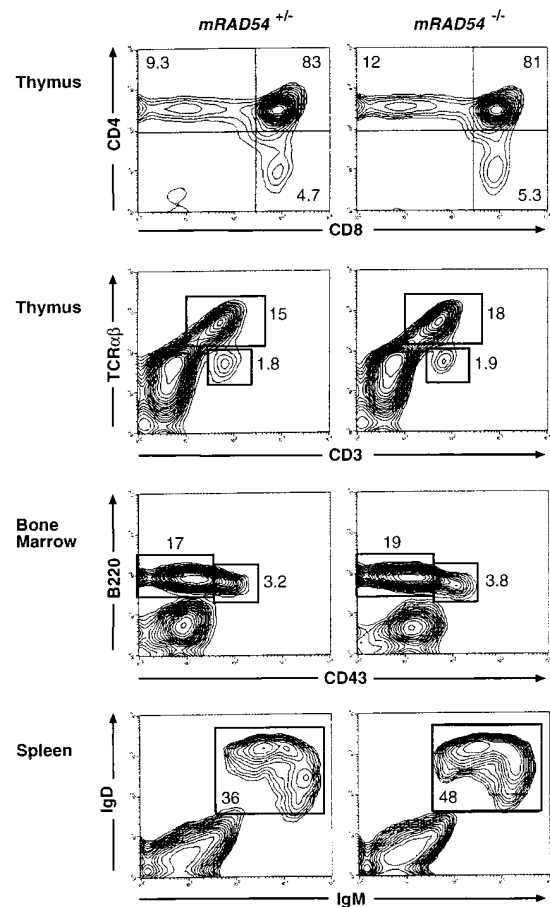

Figure 4. Analysis of V(D)J Recombination in *mRAD54* Wild-type and Mutant Mice

Flow cytometric analysis of indicated tissues in 5-week-old *mRAD54$^{+/-}$* and *mRAD54$^{-/-}$* mice. For thymus cell suspensions, the percentages of cells that express CD4 and/or CD8, as well as the percentages of CD3^{+}TCRαβ^{+} and CD3^{+}TCRαβ^{-} (i.e., TCRγδ^{+}) cells, are indicated. Bone marrow cells were stained with anti-IgM, anti-B220, and anti-CD43. IgM^{-} B cell progenitors are displayed, and the percentages of total bone marrow cells that are B220^{+}CD43^{+} pro-B cells and B220^{+}CD43^{-} pre-B cells are indicated. For spleen cell suspensions the percentages of IgM^{+}IgD^{+}B220^{+} cells are given. Shown are representative experiments from analyses of six *mRAD54$^{-/-}$* and six control mice (*mRAD54$^{+/+}$* and *mRAD54$^{+/-}$*). Data are shown as 5% probability contour plots. Dead cells were gated out based on forward and side scatter characteristics. The x and y axes are logarithmic, spanning values from 10^{0} to 10^{4}.

IgG1, IgG2a, IgG2b, IgG3, IgA, and IgE, were indistinguishable among *mRAD54$^{+/+}$*, *mRAD54$^{+/-}$*, and *mRAD54$^{-/-}$* mice (Figure 5). These results show that *mRAD54$^{-/-}$* cells are proficient in immunoglobulin isotype switching.

Discussion

The importance of the *RAD52* DNA repair pathway in the yeast S. cerevisiae has been well established. The pathway is pivotal in maintaining genomic stability by accurately repairing DSBs through homologous recombination (Game, 1993; Haber, 1995). In stark contrast, the contribution of homologous recombination to the
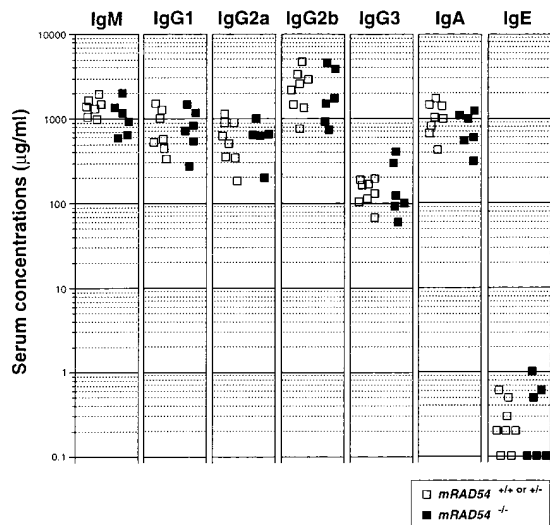
Figure 5. Analysis of Immunoglobulin Class Switch Recombination in *mRAD54* Wild-type and Mutant Mice

Serum concentrations of immunoglobulin subclasses in unimmunized 2-month-old mice, determined by sandwich ELISA. Five mice had IgE levels below the detection limit of the assay (0.1 μg/ml). Six *mRAD54*^{−/−} mice were analyzed; the control group consisted of three *mRAD54*^{+/+} and five *mRAD54*^{+/−} mice.

repair of DNA damage in mammals is currently unclear. The recent isolation of human and mouse genes with similarity to the *RAD52* group genes suggests that this DNA repair pathway is conserved in mammals. In this article, we report our use of reverse genetics to show that the mouse *RAD52* group member, *mRAD54*, is involved in homologous recombination and contributes to the repair of certain types of DNA damage. Similar results have been obtained with the use of a chicken-derived cell line (Bezzubova et al., 1997 [this issue of *Cell*]). Together, these results provide compelling genetic evidence for the functional conservation of the *RAD52* homologous recombination pathway from yeast to mammals.

The Phenotype of *mRAD54*^{−/−} ES Cells Is Consistent with a Defect in DSB Repair

S. cerevisiae strains carrying mutations in the *RAD52* group genes are sensitive to ionizing radiation. *RAD51*, *RAD52*, and *RAD54* form a distinct subset because mutations in these genes result in higher X-ray sensitivity than mutations in the other *RAD52* group genes. In addition, they have been most convincingly implicated in DSB repair (Game, 1993). Analysis of the effect of the *RAD52* group genes in mammalian cells requires mutant cell lines. To date, however, only targeted disruption of a single *mRAD51* allele in mouse ES cells has been described. Homozygous null mutants could not be isolated, either by growing *mRAD51*^{+/−} cells under elevated drug concentrations or by targeting the *mRAD51* alleles with two different selectable markers (Lim and Hasty, 1996; Tsuzuki et al., 1996). These results suggest that *mRAD51*^{−/−} cells are inviable because either mRad51-dependent DNA repair is essential in mammals or the

mammalian *RAD51* gene has an additional, yet unidentified, essential function. A number of additional *recA* analogs have been identified in yeast, and they are likely to exist in mammals as well. If these analogs do exist in mammals, they apparently are unable to take over the essential function of mammalian *RAD51*.

Here, we demonstrate that in contrast to *mRAD51*^{−/−} cells, *mRAD54*^{−/−} cells are viable (Figure 1). Disruption of one or both *mRAD54* alleles has no negative effect on the growth rate and cloning efficiency of the cells. In all of the experiments performed to date, no phenotype of heterozygous mutant *mRAD54* cells has been detected. In contrast, *mRAD54*^{−/−} cells are sensitive to ionizing radiation and MMS (Figure 2). These phenotypes are similar to those of S. cerevisiae *rad54Δ* cells. *mRAD54*^{−/−} cells display a sensitivity to ionizing radiation that is quantitatively similar to that of mouse *ATM*^{−/−} ES cells (Xu and Baltimore, 1996). *ATM*^{−/−} ES cells contain a disruption in the mouse homolog of the human *ATM* gene, which is responsible for the ataxia telangiectasia syndrome (Meyn, 1995). Whereas *RAD54* is likely to be involved directly in the repair of DNA damage, *ATM* is probably required indirectly, by mediating proper cell cycle arrest upon the induction of DNA breaks (Meyn, 1995). An abnormal G1 checkpoint function in *ATM*^{−/−} cells is reflected by the increased level of radio-resistant DNA synthesis in these cells (Barlow et al., 1996). In contrast, we observed no increase in radioresistant DNA synthesis in *mRAD54*^{−/−} cells, suggesting that this checkpoint is not affected by the absence of mRad54 (data not shown).

Analyses of DSB repair-deficient mammalian cell lines have shown that DNA end-joining, involving DNA-PK, plays a prominent role in repair of ionizing radiation–induced DNA damage (Jeggo, 1990; Jeggo et al., 1995). Defective DNA-PK$_{cs}$ activity is associated with the mouse *scid* mutation (Blunt et al., 1995; Kirchgessner et al., 1995; Peterson et al., 1995). The *scid* mutation confers a 2- to 3-fold radiosensitivity in mice and their derived tissues and cells (Biedermann et al., 1991). A similar severity in ionizing radiation sensitivity is seen in *mRAD54*^{−/−} ES cells, which appear to be impaired in homology-dependent DNA repair (see below). Interestingly, *mRAD54*^{−/−} cells are sensitive to mitomycin C (Figure 3), while mouse cells containing the *scid* mutation are not mitomycin C sensitive (Biedermann et al., 1991; Hendrickson et al., 1991). One form of DNA damage introduced by mitomycin C is an interstrand cross-link. An intermediate in the repair of these lesions is believed to be a DSB. Thus, although both DNA end-joining and homologous recombination pathways can contribute to the repair of DSBs, specialized roles for either pathway may exist (see below). Now that mutants in both repair pathways are available, the specific roles of the different DSB repair pathways in mammals can be clarified.

mRAD54 Is Involved in Homologous Recombination in Mammalian Cells

The involvement of the *RAD52* group genes in homologous recombination in S. cerevisiae and S. pombe has been clearly established. Homologous integration in S.

cerevisiae is approximately 8-fold reduced in *rad51* strains and is virtually eliminated in *rad52* strains compared to wild-type controls (Schiestl et al., 1994). S. pombe strains containing disrupted *RAD51* and *RAD54* homologs are approximately 15-fold reduced in homologous integration, while mutations in the *RAD52* homolog reduce homologous integration 2-fold (Muris et al., 1997). In general, homologous recombination in mammalian cells is relatively rare compared to random integration. The use of an isogenic targeting construct is considered to be one of the most important requirements for efficient homologous integration in mammals because DNA mismatch repair suppresses homeologous recombination (te Riele et al., 1992; de Wind et al., 1995). With the use of isogenic targeting constructs, we have shown that *mRAD54* is required for efficient homologous integration in mouse ES cells. In its absence, homologous integration is 5- to 10-fold reduced (Table 1). These results imply that gene targeting in mammalian cells can occur through a *RAD52*-like recombination pathway.

mRAD54-Deficient Mice Are Viable

To determine the biological effects of mutations in mammalian *RAD52* group genes at the whole-animal level, mice containing disrupted *RAD52* group genes are invaluable. It is difficult to uncover these effects in *mRAD51*$^{-/-}$ mice because they have an early embryonic lethal phenotype (Lim and Hasty, 1996; Tsuzuki et al., 1996). In contrast, the absence of *mRAD54* is compatible with normal mouse development. Interbreeding of F1 *mRAD54* heterozygous mutant mice results in F2 offspring in which all three genotypes are detected in a Mendelian ratio. This proves that disruption of *mRAD54* does not interfere with embryonic or neonatal development. *mRAD54*$^{-/-}$ mice are healthy, without gross abnormalities, up to at least 5 months of age. Although mRNA expression of all isolated mammalian *RAD52* group genes is increased in testis, *mRAD54*$^{-/-}$ mice produce offspring (data not shown). This shows that *mRAD54* has no essential function in meiosis, although more subtle meiotic defects have to be analyzed in more detail.

V(D)J Recombination and Class Switch Recombination Occur in *mRAD54*-Deficient Mice

The mammalian germline genome does not contain functional immunoglobulin and TCR genes. Instead, they are generated through rearrangements of gene segments during B and T cell development. In mice and humans, functional immunoglobulin and TCR genes are generated through V(D)J recombination. V(D)J recombination is initiated by a site-specific DSB, and a number of genes involved in DNA end-joining take part in processing this DSB (Jeggo et al., 1995; Gellert, 1996). Consequently, B and T cell development is arrested at an early stage in mice homozygous for a disruption of the DNA-PK component Ku80 (Nussenzweig et al., 1996; Zhu et al., 1996). In contrast, B and T cell development is normal in *mRAD54*$^{-/-}$ mice (Figure 4). This result implies

that V(D)J recombination can take place efficiently under conditions of reduced homologous recombination.

In addition to V(D)J recombination, immunoglobulin genes can undergo class-switch recombination, which controls antibody isotype. In contrast to V(D)J recombination, immunoglobulin class-switch recombination is more reminiscent of homologous recombination since it occurs between regions containing repetitive sequences (Harriman et al., 1993). However, the recombination break points are not always within the repetitive sequences (Dunnick et al., 1993). A possible relationship between homologous recombination and immunoglobulin class-switch recombination is suggested by immunolocalization experiments. Anti-hRad51 antibody staining appears to be confined to mouse B cells, switching from expression of IgM to IgG antibodies (Li et al., 1996). However, as Figure 5 shows, the concentration of antibodies of all major isotypes is similar in the serum of *mRAD54*$^{+/+}$ and *mRAD54*$^{-/-}$ mice. These results imply that mRad54 does not play a major role in immunoglobulin class-switch recombination.

The analysis of the immune system of *mRAD54*$^{-/-}$ mice presented in this article shows that immunoglobulin gene rearrangements can take place in the absence of mRad54. A role for the mammalian *RAD52*-group genes in the development of the immune system was suggested by the observation that all of these genes are highly expressed in organs of lymphoid development, such as thymus and spleen. We show here that *mRAD54* is not required for immunoglobulin and TCR gene rearrangements. Our results do not exclude the possibility that *mRAD54* function is redundant (see below) or that the absence of mRad54 results in subtle effects on the exact sequences of joints between the various immunoglobulin and TCR gene segments.

Possible Redundancy of *mRAD54* Function

At present it is unclear whether there is redundancy in any of the functions of *mRAD54*. Duplication of DNA repair genes during evolution is not uncommon. For example, there are at least two human and mouse homologs of the yeast DNA repair genes *RAD6* and *RAD23*. In addition, the *RAD52*-group genes *RAD55* and *RAD57* show sequence similarity to *RAD51*, and overexpression of *RAD51* suppresses DNA repair phenotypes of *rad55* and *rad57* cells (Hays et al., 1995; Johnson and Symington, 1995). Genes with some similarity to *RAD54* have been identified in yeast and humans (Stayton et al., 1994; Eki et al., 1996). They are clearly not as closely related to *RAD54* as are *hRAD54* and *mRAD54*, and no functional data on these genes are available. The repair and recombination phenotypes of *RAD54*-deficient S. cerevisiae and mouse cells demonstrate that some functions of *RAD54* are not redundant. However, although homologous recombination is reduced in *mRAD54*$^{-/-}$ cells, it is not completely absent. In addition, we have not yet uncovered an obvious meiotic phenotype of *mRAD54*$^{-/-}$ mice. These observations suggest that *mRAD54* homologs with specialized functions might exist.

Besides redundancy of *mRAD54* function, there could be redundancy in DNA repair pathways. The same end point may be reached by different repair pathways

through distinct mechanisms. For example, a role for DNA end-joining in the repair of ionizing radiation–induced DNA damage has been clearly demonstrated, and we show here that homologous recombination also contributes to ionizing radiation resistance. The two DNA repair pathways might differ in tissue, cell cycle, and/or damage specificity since they may have different properties. In this respect, the pathways are likely to differ in the accuracy of repair. DNA end-joining might not result in accurate repair since nucleotides at the break could be added or lost and incorrect ends might be joined. In contrast, homologous recombination ensures accurate repair because the undamaged sister chromatid or homologous chromosome is used as a template. While accurate repair seems critical for germ and stem cells, inaccurate repair could be more easily tolerated by differentiated somatic cells given that a large fraction of their genome is no longer functional.

The *RAD52* Homologous Recombination Pathway Is Functionally Conserved from Yeast to Mammals

The accumulated evidence for the functional conservation of the *RAD52* pathway in mammals is now extremely compelling. First, both Rad51 and Rad54 are highly conserved from yeast to mammals, despite their large evolutionary distance. Second, key steps in homologous recombination—the search for homology and strand exchange—are mediated in vitro by the purified yeast and human Rad51 proteins (Benson et al., 1994; Sung, 1994; Sung and Robberson, 1995; Baumann et al., 1996; Gupta et al., 1997). Third, human *RAD54* can partially complement certain DNA repair phenotypes of S. cerevisiae *rad54Δ* cells (Kanaar et al., 1996). Fourth, mouse *RAD54*$^{-/-}$ cells have a qualitatively similar phenotype compared to S. cerevisiae *rad54Δ* cells with respect to ionizing radiation and MMS sensitivity (Figure 2). Fifth, mouse *RAD54*$^{-/-}$ cells are impaired in homologous recombination (Table 1). Since *mRAD54*$^{-/-}$ mice are viable, they provide an experimental mouse model with a defined defect in a gene implicated in homology-dependent DSB repair and permit detailed assessment of the importance of this process for genetic stability, oncogenesis, and mitotic and meiotic recombination repair.

Experimental Procedures

Construction of *mRAD54* Targeting Vectors

An *mRAD54* cDNA fragment was used to screen a lambda phage and a cosmid genomic library made from a 129/Sv mouse strain (kindly provided by G. Grosveld and N. Galjart, respectively). Genomic fragments hybridizing to the *mRAD54* cDNA were subcloned in pBluescript II KS (Stratagene). The location of the intron–exon borders was determined by DNA sequencing, restriction site mapping, and PCR analysis. An approximately 9 kb EcoRI fragment encompassing exons 4, 5, and 6 and containing a unique SfuI restriction site in exon 4 was subcloned in pBluescript II KS. Three targeting vectors were made. The first was made by inserting a cassette with the neomycin resistance gene driven by the TK promoter in the unique SfuI site of exon 4. The resulting *mRAD54* allele is refered to as *mRAD54*^{307neo}. A second targeting vector was made by inserting a PGK hygromycin expression cassette in the unique exon 4 SfuI site (*mRAD54*^{307hyg}), and a third targeting vector was made by inserting a PGK puromycin cassette in the SfuI site (*mRAD54*^{307pur}).

ES Cell Culture and Electroporation

E14 ES cells (kindly provided by A. Berns, The Netherlands Cancer Institute, Amsterdam) were electroporated with the *mRAD54*^{307neo} targeting construct and cultured on gelatinized dishes as described (Zhou et al., 1995). G418 was added 24 hr after electroporation to a final concentration of 200 μg/ml, and the cells were maintained under selection for 6–8 days. Genomic DNA from individual G418-resistant clones was digested with StuI and analyzed by DNA blotting using a flanking probe. Targeted clones with the expected hybridizing StuI fragments were subsequently screened with a fragment of the neomycin resistance gene to confirm proper homologous integration. To obtain ES cell lines carrying a disruption in both *mRAD54* alleles, an *mRAD54*^{307neo}-targeted ES cell line was electroporated with the *mRAD54*^{307hyg} targeting construct. After selection with hygromycin B (200 μg/ml) for 10 days, colonies were isolated and expanded. Using the same flanking probe as was used in the *mRAD54*^{307neo} targeting experiment, cell lines containing the homologously integrated *mRAD54*^{307hyg} construct in either the wild-type or the previously targeted *mRAD54* allele were obtained. In a similar experiment with the *mRAD54*^{307pur} targeting construct, *mRAD54*$^{307neo/pur}$ double-knockout and *mRAD54*$^{307pur/+}$ single targeted cell lines were obtained. Clones were selected with puromycin (1 μg/ml) for 10 days.

Cell Survival Curves

The sensitivity of ES cells to increasing doses of DNA-damaging agents was determined by measuring their colony-forming ability. ES cells were trypsinized and counted. Various cell dilutions were aliquoted onto gelatinized 60 mm dishes, and after 12–24 hr, cells were incubated 1–2 hr in drug-containing media. Ionizing radiation sensitivity was determined by comparing the colony-forming ability of targeted ES cells after irradiation with an ^{137}Cs source. For UV irradiation (254 nm), the medium was replaced with PBS prior to exposure. Cells were grown for 7–10 days, fixed, stained, and counted. All measurements were performed in triplicate.

Rescue of *mRAD54*$^{-/-}$ Cells by cDNA Expression

The *mRAD54* cDNA was subcloned in pPGK-p(A). This cDNA expression construct was coelectroporated with a PGK puromycin plasmid in *mRAD54*$^{307neo/hyg}$ cells. Clones were selected with puromycin (1 μg/ml) for 10 days. Integration of the cDNA construct and mRad54 expression were confirmed by DNA blotting and immunoblot analysis, respectively.

Homologous Targeting of *RB* and *CSB* Loci

Targeting and subsequent analysis of the *RB* and *CSB* loci in E14, *mRAD54*$^{+/-}$, and *mRAD54*$^{-/-}$ ES cells were done as described previously (Zhou et al., 1995). The targeting constructs *129RB-hyg* and *129RB-puro* were kindly provided by H. te Riele (The Netherlands Cancer Institute, Amsterdam). The targeting construct *CSB-pur* was obtained by inserting a PGK puromycin expression cassette in an unique XhoI site of an approximately 7 kb genomic fragment of the mouse *CSB* gene (van der Horst et al., 1997). Targeted integration in the *RB* and *CSB* loci was distinguished from random integration by DNA blot analysis using appropriate probes flanking the targeting constructs (data not shown).

Generation of *mRAD54* Mutant Mice

Cells of *mRAD54*^{307neo}-targeted clones were karyotyped, and ES cells from clones with 40 chromosomes were used for injection into C57BL/6 blastocysts (Zhou et al., 1995). Male chimeric mice were mated with C57BL/6 females and found to transmit the disrupted *mRAD54* allele to the germline. *mRAD54*$^{-/-}$ mice were obtained by intercrossing F1 heterozygotes. Genotyping was performed by DNA blot analysis with a flanking probe or PCR analysis or both.

Flow Cytometric Analysis

Single-cell suspensions from lymphoid tissues were prepared and stained with monoclonal antibodies, and 3×10^4 cells were scored with a FACScan flow cytometer (Becton Dickinson, Sunnyvale, CA) (Hendriks et al., 1996). Antibodies obtained from Pharmingen (San

Diego, CA) included phycoerythrin (PE)–conjugated anti-CD4, anti-CD25, anti-CD43, anti-CD5, biotinylated anti-IgM, anti-CD8, fluorescein isothiocyanate–conjugated anti-B220/RA3–6B2, and anti-CD3. Phycoerythrin-conjugated anti-IgD was purchased from Southern Biotechnology Associates (Birmingham, AL). Purified monoclonal antibodies anti-Thy1/59AD22, anti-TCRαβ/H57597, and anti-TCRγδ/GL3 were conjugated to biotin using standard procedures. TriColor-conjugated streptavidin (Caltag Laboratories, CA) was used as a secondary antibody.

Serum Immunoglobulin Detection
Levels of immunoglobulin subclasses in serum were measured by sandwich ELISA using unlabeled anti-mouse immunoglobulin subclass-specific antibodies (Southern Biotechnology) as capture reagents. Serially diluted sera were incubated for 3 hr. Subsequently, peroxidase-labeled anti-mouse immunoglobulin subclass-specific antibodies and azino-bis-ethylbenz-thiazoline-sulfonic acid were added.

References

Barlow, C., Hirotsune, S., Paylor, R., Liyanage, M., Eckhaus, M., Collins, F., Shiloh, Y., Crawley, J.N., Ried, T., Tagle, D., et al. (1996). *Atm*-deficient mice: a paradigm of ataxia telangiectasia. Cell *86*, 159–171.

Baumann, P., Benson, F.E., and West, S.C. (1996). Human Rad51 protein promotes ATP-dependent homologous pairing and strand transfer reactions in vitro. Cell *87*, 757–766.

Benson, F.E., Stasiak, A., and West, S.C. (1994). Purification and characterization of the human Rad51 protein, an analogue of *E. coli* RecA. EMBO J. *13*, 5764–5771.

Bezzubova, O., Silbergleit, A., Yamaguchi-Iwai, Y., Takeda, S., and Buerstedde, J.-M. (1997). Reduced X-ray resistance and homologous recombination frequencies in a *RAD54*⁻/⁻ mutant of the chicken DT40 cell line. Cell *89*, this issue.

Biedermann, K.A., Sun, J., Giaccia, A.J., Tosto, L.M., and Brown, J.M. (1991). *scid* mutation in mice confers hypersensitivity to ionizing radiation and a deficiency in DNA double-strand break repair. Proc. Natl. Acad. Sci. USA *88*, 1394–1397.

Blunt, T., Finnie, N.J., Taccioli, G.E., Smith, G.C.M., Demengeot, J., Gottlieb, T.M., Mizuta, R., Varghese, A.J., Alt, F.W., Jeggo, P.A., et al. (1995). Defective DNA-dependent protein kinase activity is linked to V(D)J recombination and DNA repair defects associated with the murine *scid* mutation. Cell *80*, 813–823.

Clever, B., Interthal, H., Schmuckli-Maurer, J., King, J., Sigrist, M., and Heyer, W.-D. (1997). Recombinational repair in yeast: functional interactions between Rad51 and Rad54 proteins. EMBO J., in press.

de Wind, N., Dekker, M., Berns, A., Radman, M., and te Riele, H. (1995). Inactivation of the mouse *Msh2* gene results in mismatch repair deficiency, methylation tolerance, hyperrecombination, and predisposition to cancer. Cell *82*, 321–330.

Dunnick, W., Hertz, G.Z., Scappino, L., and Gritzmacher, C. (1993). DNA sequences at immunoglobulin switch region recombination sites. Nucleic Acids Res. *21*, 365–372.

Eisen, J.A., Sweder, K.S., and Hanawalt, P.C. (1995). Evolution of the SNF2 family of proteins: subfamilies with distinct sequences and functions. Nucleic Acids Res. *23*, 2715–2723.

Eki, T., Naitou, M., Hagiwara, H., Abe, M., Ozawa, M., Sasanuma, S., Sasanuma, M., Tsuchiya, Y., Shibata, T., Watanabe, K., Ono, A., Yamazaki, M.A., Tashiro, H., Hanaoka, F., and Murakami, Y. (1996). Fifteen open reading frames in a 30.8 kb region of the right arm of chromosome VI from *Saccharomyces cerevisiae*. Yeast *12*, 177–190.

Game, J.C. (1993). DNA double-strand breaks and the *RAD50-RAD57* genes in *Saccharomyces*. Semin. Cancer Biol. *4*, 73–83.

Gellert, M. (1996). A new view of V(D)J recombination. Genes to Cells *1*, 269–275.

Gupta, R.C., Bazemore, L.R., Golub, E.I., and Radding C.M. (1997). Activities of human recombination protein Rad51. Proc. Natl. Acad. Sci. USA *94*, 463–468.

Haber, J.E. (1995). *In vivo* biochemistry: physical monitoring of recombination induced by site-specific endonucleases. Bioessays *17*, 609–620.

Hardy, R.R., Carmack, C.E., Shinton, S.A., Kemp, J.D., and Hayakawa, K. (1991). Resolution and characterization of pro-B and pre-B cell stages in normal mouse bone marrow. J. Exp. Med. *173*, 1213–1225.

Harriman, W., Völk, H., Defranoux, N., and Wabl, M. (1993). Immunoglobulin class switch recombination. Annu. Rev. Immunol. *11*, 361–384.

Hays, S., Firmich, A.A., and Berg, P. (1995). Complex formation in yeast double-strand break repair: participation of Rad51, Rad55, and Rad57 proteins. Proc. Natl. Acad. Sci. USA *92*, 6925–6929.

Hendrickson, E.A., Qin, X.-Q., Bump, E.A., Schatz, D.G., Oettinger, M., and Weaver, D.T. (1991). A link between double-strand break-related repair and V(D)J recombination: the *scid* mutation. Proc. Natl. Acad. Sci. USA *88*, 4061–4065.

Hendriks, R.W., de Bruijn, M.F.T.R., Maas, A., Dingjan, G.M., Karis, A., and Grosveld, F. (1996). Inactivation of Btk by insertion of lacZ reveals defects in B cell development only past the pre-B cell stage. EMBO J. *15*, 4862–4872.

Jeggo, P.A. (1990). Studies on mammalian mutants defective in rejoining double-strand breaks in DNA. Mutat. Res. *239*, 1–16.

Jeggo, P.A., Taccioli, G.E., and Jackson, S.P. (1995). Menage à trois: double strand break repair, V(D)J recombination and DNA-PK. Bioessays *17*, 949–957.

Jiang, H., Xie, Y., Houston, P., Stemke-Hale, K., Mortensen, U.H., Rothstein, R., and Kodadek, T. (1996). Direct association between the yeast Rad51 and Rad54 recombination proteins. J. Biol. Chem. *271*, 33181–33186.

Johnson, R.D., and Symington, L.S. (1995). Functional differences and interactions among the putative RecA homologs Rad51, Rad55, and Rad57. Mol. Cell. Biol. *15*, 4843–4850.

Kanaar, R., Troelstra, C., Swagemakers, S.M.A., Essers, J., Smit, B., Franssen, J.-H., Pastink, A., Bezzubova, O.Y., Buerstedde, J.-M., Clever, B., Heyer, W.-D., and Hoeijmakers, J.H.J. (1996). Human and mouse homologs of the *Saccharomyces cerevisiae RAD54* DNA repair gene: evidence for functional conservation. Curr. Biol. *6*, 828–838.

Kingston, R.E., Bunker, C.A., and Imbalzano, A.N. (1996). Repression and activation by multiprotein complexes that alter chromatin structure. Genes Dev. *10*, 905–920.

Kirchgessner, C.U., Patil, C.K., Evans, J.W., Cuomo, C.A., Fried, L.M., Carter, T., Oettinger, M.A., and Brown, J.M. (1995). DNA-dependent protein kinase (p350) as a candidate gene for the murine scid defect. Science *267*, 1178–1183.

Li, M.-J., Peakman, M., Golub, E., Reddy, G., Ward, D., Radding, C., and Maizels, N. (1996). Rad51 expression and localization in B cells carrying out class switch recombination. Proc. Natl. Acad. Sci. USA *93*, 10222–10227.

Lim, D., and Hasty, P. (1996). A mutation in mouse *rad51* results in an early embryonic lethal phenotype that is suppressed by a mutation in *p53*. Mol. Cell. Biol. *16*, 7133–7143.

Meyn, M.S. (1995). Ataxia-telangiectasia and cellular responses to DNA damage. Cancer Res. *55*, 5991–6001.

Mombaerts, P., Iacomini, J., Johnson, R.S., Herrup, K., Tonegawa, S., and Papaioannou, V.E. (1992). RAG-1-deficient mice have no mature B and T lymphocytes. Cell *68*, 869–877.

Muris, D.F.R., Vreeken, K., Carr, A.M., Murray, J.M., Smit, C., Lohman, P.H.M., and Pastink, A. (1996). Isolation of the *Schizosaccharomyces pombe RAD54* homologue, *rhp54+*, a gene involved in the repair of radiation damage and replication fidelity. J. Cell Sci. *109*, 73–81.

Muris, D.F.R., Vreeken, K., Schmidt, H., Ostermann, K., Clever, B., Lohman, P.H.M., and Pastink, A. (1997). Homologous recombination in the fission yeast *Schizosaccharomyces pombe*: different requirements for the *rhp51+*, *rhp54+* and *rad22+* genes. Curr. Genet., in press.

Nussenzweig, A., Chen, C., da Costa Soares, V., Sanchez, M., Sokol, K., Nussenzweig, M.C., and Li, G.C. (1996). Requirement for Ku80 in growth and immunoglobulin V(D)J recombination. Nature *382*, 551–555.

Ogawa, T., Yu, X., Shinohara, A., and Egelman, E.H. (1993). Similarity of the yeast RAD51 filament to the bacterial RecA filament. Science *259*, 1896–1899.

Peterson, S.R., Kurimasa, A., Oshimura, M., Dynan, W.S., Bradbury, E.M., and Chen, D.J. (1995). Loss of the catalytic subunit of DNA-dependent protein kinase in DNA double-strand break repair mutant mammalian cells. Proc. Natl. Acad. Sci. USA *92*, 3171–3174.

Petrini, J.H.J., Bressan, D.A., and Yao, M.S. (1997). The *RAD52* epistasis group in mammalian double strand break repair. Semin. Immunol., in press.

Roth, D.B., Lindahl, T., and Gellert, M. (1995). How to make ends meet. Curr. Biol. *5*, 496–499.

Schiestl, R.H., Zhu, J., and Petes, T.D. (1994). Effect of mutations in genes affecting homologous recombination on restriction enzyme-mediated and illegitimate recombination in *Saccharomyces cerevisiae*. Mol. Cell. Biol. *14*, 4493–4500.

Shinkai, Y., Rathbun, G., Lam, K.P., Oltz, E.M., Stewart, V., Mendelsohn, M., Charron, J., Datta, M., Young, F., Stall, A.M., et al. (1992). RAG-2–deficient mice lack mature lymphocytes owing to inability to initiate V(D)J rearrangement. Cell *68*, 855–867.

Stayton, C.L., Dabovic, B., Gulisano, M., Gecz, J., Broccoli, V., Giovanni, S., Bossoloasco, M., Monaco, L., Rastan, S., Boncinelli, E., et al. (1994). Cloning and characterization of a new human Xq13 gene, encoding a putative helicase. Hum. Mol. Genet. *3*, 1957–1964.

Sung, P. (1994). Catalysis of ATP-dependent homologous DNA pairing and strand exchange by yeast Rad51 protein. Science *265*, 1241–1243.

Sung, P., and Robberson, D.L. (1995). DNA strand exchange mediated by a RAD51–ssDNA nucleoprotein filament with polarity opposite to that of RecA. Cell *82*, 453–461.

te Riele, H., Maandag, E.B., and Berns, A. (1992). Highly efficient gene targeting in embryonic stem cells through homologous recombination with isogenic DNA constructs. Proc. Natl. Acad. Sci. USA *89*, 5128–5132.

Tomasz, M., Lipman, R., Chowdary, D., Pawlak, J., Verdine, G., and Nakanishi, K. (1987). Isolation and structure of covalent cross link between mitomycin C and DNA. Science *235*, 1204–1208.

Tsuzuki, T., Fujii, Y., Sakumi, K., Tominaga, Y., Nakao, K., Sekiguchi, M., Matsushiro, A., Yoshimura, Y., and Morita, T. (1996). Targeted disruption of the *Rad51* gene leads to lethality in embryonic mice. Proc. Natl. Acad. Sci. USA *93*, 6236–6240.

van der Horst, G.T.J., van Steeg, H., Berg, R.J.W., de Wit, J., van Gool, A.J., Weeda, G., Morreau, H., Beems, R.B., van Kreijl, C.F., and de Gruijl, F.R., et al. (1997). Defective transcription-coupled repair in the Cockayne syndrome B mice is associated with skin cancer predisposition. Cell *89*, in press.

Xu, Y., and Baltimore, D. (1996). Dual roles of ATM in the cellular response to radiation and in cell growth control. Genes Dev. *10*, 2401–2410.

Zhou, X.Y., Morreau, H., Rottier, R., Davis, D., Bonten, E., Gillmans,

N., Wenger, D., Grosveld, F.G., Doherty, P., Suzuki, K., et al. (1995). Mouse model for the lysozomal disorder galactosialidosis and correction of the phenotype with overexpressing erythroid precursor cells. Genes Dev. *9*, 2623–2634.

Zhu, C., Bogue, M.A., Lim, D.-S., Hasty, P., and Roth, D.B. (1996). Ku86-deficient mice exhibit severe combined immunodeficiency and defective processing of V(D)J recombination intermediates. Cell *86*, 379–389.